

Ab-initio electronic and optical properties of low dimensional systems: From single particle to many-body approaches

M. Palumbo^{a,*}, M. Bruno^a, O. Pulci^a, E. Luppi^b, E. Degoli^c, S. Ossicini^c, R. Del Sole^a

^a *European Theoretical Spectroscopy Facility (ETSF), CNR-INFM, Institute for Statistical Mechanics and Complexity, CNISM, Dipartimento di Fisica, Università di Roma, 'Tor Vergata', via della Ricerca Scientifica 1, 00133 Roma, Italy*

^b *European Theoretical Spectroscopy Facility (ETSF), Laboratoire des Solides Irradiés, École Polytechnique, F-91128 Palaiseau, France*

^c *INFM-S³ "nanoStructures and bioSystems at Surfaces", Dipartimento di Scienze e Metodi dell'Ingegneria, via G. Amendola 2, Università di Modena e Reggio Emilia, Italy*

Available online 16 December 2006

Abstract

Low dimensional systems, such as nanodots, nanotubes, nanowires, have attracted great interest in the last years, due to their possible application in nanodevices. It is hence very important to describe accurately their electronic and optical properties within highly reliable and efficient ab-initio approaches. Density functional theory (DFT) has become in the last 20 years the standard technique for studying the ground-state properties, but this method often shows significant deviations from the experiment when electronic excited states are involved. The use of many-body Green's functions theory, with DFT calculations taken as the zero order approximation, is today the state-of-the-art technique for obtaining quasi-particle excitation energies and optical spectra. In this paper we will present the current status of this theoretical and computational approach, showing results for different kinds of low dimensional systems.

© 2007 Elsevier B.V. All rights reserved.

Keywords: Ab-initio; Excited states

1. Introduction

Semiconductor device fabrication shows a remarkable trend towards miniaturization, driven by many scientific and technological innovations. The size of device components is now reaching the nanometric scale, which is the actual fabrication technological limit. This limitation could be overcome by substituting traditional inorganic semiconductor components with single nanostructures, such as nanowires, nanotubes, or organic molecules. It is therefore important to study these systems in order to understand their properties and possible electronic and optoelectronic applications. Theoretical calculations can help in the interpretation of experimental results, and, more importantly, may be useful in predicting structural, electronic, optical, and transport properties to help to realize more efficient devices. Density functional theory (DFT) [1] is a single-parti-

cle approach successfully used to calculate the ground-state electronic properties of many-electron systems. However, when physical phenomena involving excited states are studied, it is necessary to include many-body effects, through Green's function theory. The use of many-body perturbation theory [2], with DFT calculations as zero order approximation, is nowadays the state-of-the-art to obtain quasi-particle excitation energies and dielectric response in an increasing number of systems, from bulk materials to surfaces and nanostructures. A general discussion of the theoretical framework will be presented in the next sections, while some examples of applications to systems of different dimensionality will be given in the last section.

2. Theoretical background

In this section we will briefly discuss the main equations of the theoretical ab-initio framework used here, in order to resume the different levels of approximations. First,

* Corresponding author.

E-mail address: maurizia.palumbo@roma2.infn.it (M. Palumbo).

through a DFT calculation within local density approximation (LDA) [2,3], with the use of norm-conserving pseudo-potentials [4], the geometrical structure of the relaxed ground-state configuration of the system has been obtained, solving self-consistently the one-particle Kohn–Sham (KS) equations [5]:

$$\left[-\frac{1}{2}\nabla^2 + V_{\text{ext}}(\mathbf{r}) + V_{\text{H}}(\mathbf{r}) + V_{\text{xc}}(\mathbf{r}) \right] \cdot \varphi_i(\mathbf{r}) = \epsilon_i \varphi_i(\mathbf{r}), \quad (1)$$

where V_{ext} is the external potential due to the ions, V_{H} is the Hartree potential, V_{xc} is the exchange–correlation potential.

Being the DFT a ground-state theory, there is no rigorous justification to interpret the KS eigenvalues ϵ_i as electron addition or removal energies. As a consequence, the calculated DFT–LDA electronic band gaps of semiconductors and insulators severely underestimate the experimental ones [6]. Moreover it is well known [6] that also the optical spectra calculated at the DFT–LDA level, not only underestimate peak energies, but miss relative peak intensities. In order to give a proper description of the electronic excited states of a system, the Green’s function formalism can be used [6].

The quasi-particle excitation energies are the poles of the one-particle Green function and are determined as solutions of the quasi-particle equation which is similar to the Kohn–Sham equation, where a non-Hermitian, non-local, energy dependent self-energy operator Σ [7] replaces the exchange–correlation potential. In practical calculations the self-energy is approximated by the product of the Kohn–Sham Green function G times the screened Coulomb interaction W obtained within the random phase approximation (RPA): $\Sigma = iGW$ (see Ref. [8] and references therein).

Moreover, a first-order perturbative solution of quasi-particle equation is used, with respect to $\Sigma - V_{\text{xc}}$. In this way the quasi-particle energies are obtained as

$$\epsilon_i^{\text{QP}} = \epsilon_i^{\text{LDA}} + \frac{1}{1 + \beta_i} \langle \varphi_i^{\text{LDA}} | \Sigma(\epsilon_i^{\text{LDA}}) - V_{\text{xc}}^{\text{LDA}} | \varphi_i^{\text{LDA}} \rangle, \quad (2)$$

where β_i is the linear coefficient in the energy expansion of Σ .

Once the quasi-particle energies and wavefunctions are known we are able to evaluate the macroscopic dielectric function $\epsilon_{\text{M}}(\omega)$ which can be compared to the experimental evidence. Indeed $\epsilon_{\text{M}}(\omega)$ is defined as [9,10]

$$\epsilon_{\text{M}}(\omega) = \lim_{q \rightarrow 0} \frac{1}{\epsilon_{\mathbf{G}=0, \mathbf{G}'=0}^{-1}(\mathbf{q}, \omega)}. \quad (3)$$

This formula relies on the fact that, although in an inhomogeneous material the macroscopic field varies with frequency ω and has a Fourier component of vanishing wavevector, the microscopic field varies with the same frequency but with different wavevectors $q + G$. These microscopic fluctuations induced by the external perturbation are at the origin of the local-field effects (LF) and reflect the spatial anisotropy of the material. The evaluation of $\epsilon_{\text{M}}(\omega)$

within the linear response theory, in the independent particle approximation leads to the RPA dielectric function.

At this level, even if GW corrections are included, still no good agreement with the experimental results is found. In particular one finds optical spectra with peaks often at higher energies than the experimental ones and with wrong relative intensities.

In order to describe correctly the spectroscopic processes, where electron–hole pairs are created, the inclusion of the self-energy corrections alone, to the DFT eigenvalues, and the inclusion of local-field effects, are still not enough. The solution of the Bethe–Salpeter equation (BSE), where the coupled electron–hole excitations are included [6], is required. Detailed discussions about this equation are already present in the literature [6]; here, we just recall that its solution involves the study of the following excitonic Hamiltonian:

$$\begin{aligned} H_{\text{exc}}^{(n_1, n_2), (n_3, n_4)} &= (E_{n_2} - E_{n_1}) \delta_{n_1, n_3} \delta_{n_2, n_4} - i(f_{n_2} - f_{n_1}) \\ &\times \int d\mathbf{r}_1 d\mathbf{r}'_1 d\mathbf{r}_2 d\mathbf{r}'_2 \phi_{n_1}(\mathbf{r}_1) \phi_{n_2}^*(\mathbf{r}'_1) \\ &\times \Xi(\mathbf{r}_1, \mathbf{r}'_1, \mathbf{r}_2, \mathbf{r}'_2) \phi_{n_3}^*(\mathbf{r}_2) \phi_{n_4}(\mathbf{r}'_2), \end{aligned}$$

where n_i refer to energy indexes of Kohn–Sham states. The kernel Ξ contains two contributions: \bar{v} , which is the bare coulomb interaction where the long range part corresponding to vanishing wave vector is not included (which describes local-field effects), and W , the attractive screened coulomb electron–hole interaction. Using this formalism and considering only the resonant part of the excitonic Hamiltonian [6], the macroscopic dielectric function comes out to be

$$\epsilon_{\text{M}}(\omega) = 1 + \lim_{q \rightarrow 0} v(\mathbf{q}) \sum_{\lambda} \frac{\left| \sum_{v, c; \mathbf{k}} \langle v, \mathbf{k} - \mathbf{q} | e^{-i\mathbf{q}\mathbf{r}} | c, \mathbf{k} \rangle A_{\lambda}^{(v, c; \mathbf{k})} \right|^2}{(E_{\lambda} - \omega)}. \quad (4)$$

In Eq. (4) the dielectric function, differently from the RPA approximation, is given by a mixing of single-particle transitions weighted by the excitonic eigenvectors A_{λ} . Moreover the excitation energies in the denominator are changed from $\epsilon_c - \epsilon_v$ (single-particle energy transitions) to E_{λ} which are the excitonic eigenvalues.

3. Applications: from surfaces to nanostructures

In this section, we will describe how many-body effects influence the electronic and optical properties of three systems of different dimensionality: the (100) surface of diamond, the Ge_9H_{12} [100] germanium nanowire and the $\text{Si}_{10}\text{H}_{16}$ nanodots.

3.1. The reflectance anisotropy spectrum of (100) surface of diamond

The C(100) surface is an emblematic case, which demonstrates the importance to introduce many-body effects

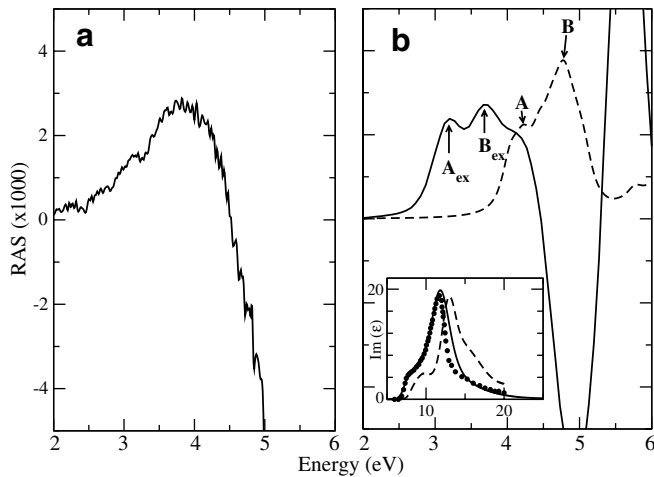


Fig. 1. Panel (a): Experimental RA spectrum of C(100) (solid line), see Ref. [13] for more details. Panel (b): Theoretical RA spectrum (solid line), with excitonic, self-energy (GW) and local-field (LF) effects included. Theoretical RA spectrum (dashed line) with only self-energy (GW) corrections. The labels A_{ex} and B_{ex} indicate the two bound excitons corresponding to the two one-particle transitions between the π and π^* surface states, indicated with labels A and B. Inset of Panel (b): $\epsilon_2(\omega)$ of bulk diamond: experimental curve (dots), theoretical curve with GW + LF + EXC (solid curve), and including only GW corrections (dashed curve).

for an appropriate description of the measured optical properties. In fact, as can be seen from Fig. 1, the theoretical optical spectrum, obtained at the independent-quasi-particle (IQP-RPA) level (dashed curve, panel (b)), dramatically differs from the experiments¹ (solid curve, panel (a)), because the two peaks A and B are at too high an energy so that the strong negative contribution above 4.5 eV, is not reproduced. Inclusion of the excitonic effects has a very strong effect, and yields good agreement with the experiment (see the solid curve, panel (b)). Two strongly bound excitons (A_{ex} and B_{ex}), with calculated energy peaks in close agreement with the experimental structures at 3.1 and 3.8 eV, develop from the corresponding one-particle transitions (A and B). Furthermore the deep negative feature of the reflectance anisotropy (RA) spectrum above the electronic gap, is well reproduced. Finally we underline that the calculated binding energy of the two excitons is 0.9 eV, the largest ever found for semiconductor surfaces.

3.2. Germanium nanowires

In Fig. 2, we report the imaginary part of the dielectric function of Ge [100] wire with diameter of 0.4 nm for light polarized along the growth axis and perpendicular to it. These spectra are calculated for an inter-wire distance

¹ The reflectance anisotropy spectroscopy (RAS) [11,12] is an experimental technique used nowadays as a practical tool to characterize surfaces and interfaces. It is a high resolution and non-destructive optical technique that achieves surface sensitivity by measuring the difference in reflectivity of normal incident light, for two perpendicular directions on a surface. This geometry leads to a cancellation of the bulk contribution for cubic crystals [12].

(minimum distance between wire surfaces), equal to $D = 10 \text{ \AA}$, which leads to nearly isolated wires. The first row of each panel shows the optical spectrum obtained at the RPA level, confirming essentially the results obtained in Ref. [14]. The second row shows how the dielectric response is modified by taking into account the inhomogeneity of the system (RPA + LF). In particular, including the so called local-field effects, we observe a small change of the optical spectrum for light polarized along the wire axis, while we point out an important intensity reduction for the perpendicular light polarization (right panel). The reason that RPA, without LF, fails for \perp polarization is due to the depolarization effect [15] which is created by the polarization charges induced in the system. The depolarization is accounted only if LFs are included, and is responsible of the suppression of the low energy absorption in the \perp direction, rendering the wire almost transparent below 8 eV. A similar anisotropic behaviour, found in other first-principles calculations on nanotubes [15,16] and nanowires [17,18], has been observed in the optical absorption of carbon nanotubes [19], in the photoluminescence spectra of porous silicon [20] and in the optical gain in silicon elongated nanodots [21].

The third row of each panel reports both the absorption spectra when self-energy corrections (GW) and self-energy, local-field and excitonic effects (GW + LF + EXC) are taken into account. For perpendicular light polarization (right panel), the GW + LF + EXC spectrum is rather similar to the RPA + LF curve, whereas for parallel light polarization, a big transfer of the oscillator strength to the low energy peaks is observed, due to the presence of strongly bound excitons, together with a reduction of the Sommerfeld factor above the electronic gap (as predicted in simplified models [22,23]). Large exciton binding energies, due to the larger overlap of electron and hole wavefunctions inside the wire, come out.

Regarding this GeNW, we aim to discuss also how the inter-wire distance can strongly affect the optical absorption. This is a point of particular importance since experimentally, very often, the individual wires are close packed and can interact with each other via long-range forces induced by the excitations.

In Fig. 3 are reported the theoretical optical spectra calculated for a solid of interacting nanowires with inter-wire distance $D_{w-w} = 3 \text{ \AA}$, using the same notation of Fig. 2. Looking at the top and central row, we first note that the depolarization effect is much weaker: the packing effect makes the wire, no more transparent for light polarized perpendicular to the axis. Furthermore, reducing the inter-wires distance, an important effect on the GW corrections and on the electron-hole interaction are observable. In fact, comparing the lower row of Fig. 3 with the corresponding one of Fig. 2 we can observe a reduction of the opening of the DFT gaps, due to the GW corrections, and also a reduction of the excitonic binding energy.

The spectra for light polarized along the wire axis, after the inclusion of all many-body effects are quite similar to

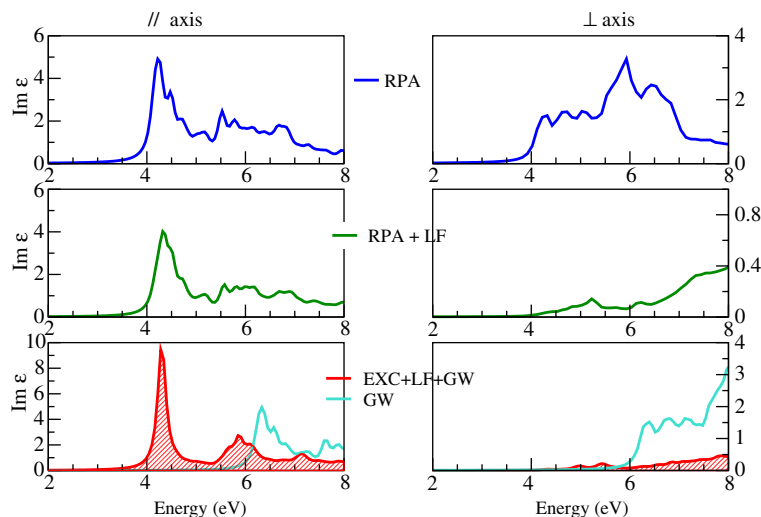


Fig. 2. Imaginary part of the dielectric function of an isolated [100] GeNW ($D = 0.4$ nm). Left panels: light polarized along the wire axis; right panels: light polarized perpendicularly to this axis. The reader should note the different scale of the vertical axes in the panels. The dashed areas correspond to the calculations including all many-body effects.

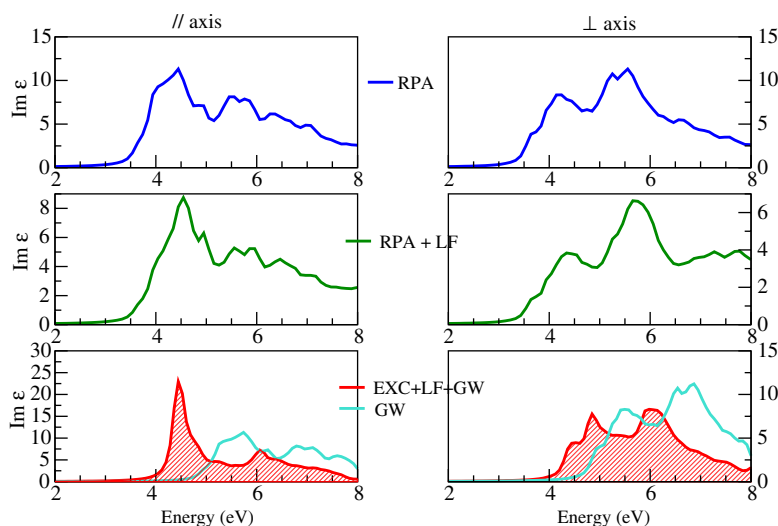


Fig. 3. As in Fig. 2 but for a solid of interacting nanowires.

those shown in Fig. 2. This is probably due to the lack of local-field effects and to a strong confinement of excitons within each wire, with respect to the DFT electron states. As a consequence, excitons in different wires behave quite independently for this light polarization.

3.3. Silicon nanocrystals

The importance of many-body effects in the study of low dimensional systems is well exemplified by the emission and absorption spectra of Silicon nanocrystals (Si-nc). These have attracted increasing interest because of the possibility to engineer luminescing transitions in an otherwise indirect gap material [24]. It is generally accepted that the quantum

confinement, caused by the restricted (nanometric) size, is essential for the visible light emission in Si nanostructures.

Still the exact role of defects, doping, and interface structure in the photoluminescence (PL) spectra have to be clarified. In particular, the PL properties of embedded Si-nc in SiO₂ suggest that oxygen induces important modifications in the electronic and optical properties of silicon nanocrystals [25]. In Fig. 4 we show the calculated absorption and emission spectra for a small Si nanocluster, the Si₁₀H₁₆, and the corresponding optical spectra in the case of Si₁₀H₁₄O, where two hydrogen atoms have been substituted by a oxygen atom in a bridge configuration (see Fig. 5). Absorption and emission are calculated in the geometries corresponding to ground and excited states, respectively, where the excited state corresponds to the

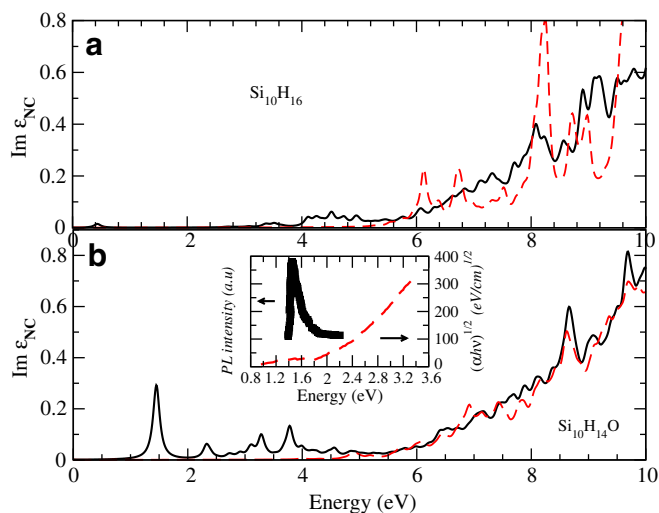


Fig. 4. (a) Imaginary part of the dielectric function of $\text{Si}_{10}\text{H}_{16}$ nanocluster. Solid line: emission; dashed line: absorption. (b) Imaginary part of the dielectric function of $\text{Si}_{10}\text{H}_{14}\text{O}$ nanocluster. Solid line: emission; dashed line: absorption. Inset: experiment by Ma et al. [25].

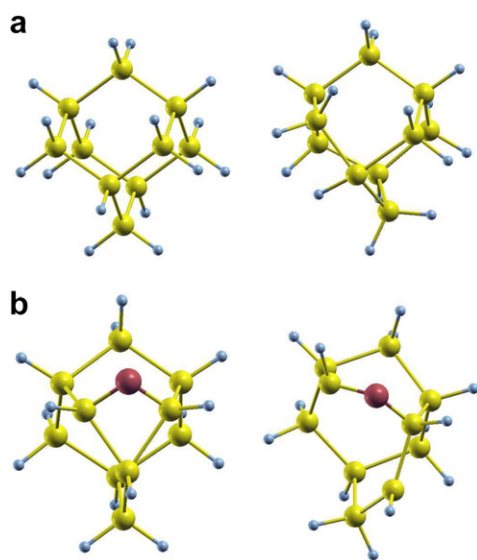


Fig. 5. Geometries of (a) $\text{Si}_{10}\text{H}_{16}$ and (b) $\text{Si}_{10}\text{H}_{14}\text{O}$ nanoclusters. Left: ground-state geometries; right: excited state geometries.

electronic configuration in which the highest occupied single-particle state (HOMO) contains a hole (h), while the lowest unoccupied single-particle state (LUMO) contains the corresponding electron (e).

Excitonic, local-field and self-energy effects are included. A strong photoluminescence peak appears around 1.5 eV in the case of $\text{Si}_{10}\text{H}_{14}\text{O}$, due to a bound exciton with a large binding energy of ~ 2 eV. The resulting emission spectrum well compares with the experimental spectrum of Ma et al. [25] shown in the inset. Our results suggests that the presence of a Si–O–Si bridge bond at the surface of Si-nc can explain the nature of luminescence in Si nanocrystals embedded in SiO_2 .

4. Conclusions

In the present paper we have summarized the ab-initio theoretical and computational scheme, obtained from a combination of density functional and many-body perturbation theories, which nowadays allow the calculation of both ground and excited state properties of many materials. We have illustrated the quasi-particle equation and the GW approximation which yields quite accurate results in many materials, and the Bethe–Salpeter equation needed to describe the electron–hole dynamics. Some examples, where many-body effects strongly influence the dielectric response have also been given. As a rule, the optical properties of low dimensional systems like surfaces, thin quantum wires and small nanocrystals are greatly affected by the electron–hole interaction and strongly depend on shape and size.

Acknowledgements

This work was funded in part by the EU’s Sixth Framework Programme through the Nanoquanta Network of Excellence (NMP4-CT-2004-500198), and by MIUR through NANOSIM and PRIN 2005. We acknowledge the CINECA CPU time granted by INFN. We are gratefully to Andrea Marini and Valerio Olevano for useful discussions. The many-body calculations on the germanium nanowires have been performed using the code SELF [26]. Excitonic spectra on Si-nc have been calculated with the code EXC <http://www.bethe-salpeter.org/>.

References

- [1] P. Hohenberg, W. Kohn, *Physical Review* 136 (1964) B864.
- [2] D.M. Ceperley, B.J. Alder, *Physical Review Letters* 45 (1980) 566.
- [3] X. Gonze, J.M. Beuken, R. Caracas, F. Detraux, M. Fuchs, G.M. Rignanese, L. Sindic, M. Verstraete, G. Zerah, F. Jollet, M. Torrent, A. Roy, M. Mikami, P. Ghosez, J.Y. Raty, D.C. Allan, *Computation Materials Science* 25 (2002) 478.
- [4] N. Troullier, J.L. Martins, *Physical Review B* 43 (1991) 19993.
- [5] W. Kohn, L.J. Sham, *Physical Review* 140 (1965) A1113.
- [6] G. Onida, L. Reining, A. Rubio, *Reviews of Modern Physics* 74 (2002) 601.
- [7] L. Hedin, *Physical Review* 139 (1965) A796.
- [8] F. Aryasetiawan, O. Gunnarsson, *Reports on Progress in Physics* 61 (1998) 237.
- [9] S.L. Adler, *Physical Review* 126 (1962) 413.
- [10] N. Wiser, *Physical Review* 129 (1962) 62.
- [11] D.E. Aspnes, J.F. Harbison, A.A. Studna, L.T. Florez, *Journal of Vacuum Science and Technology A* 6 (1988) 1327.
- [12] P. Chiaradia, R.D. Sole, *Surface Review and Letters* 6 (1999) 517.
- [13] M. Palumbo, O. Pulci, R.D. Sole, A. Marini, M.S.S.R. Haines, K.H. Williams, D.S. Martin, P. Weightman, J.E. Butler, *Physical Review Letters* 94 (2005) 087404.
- [14] A.N. Kholod, V.L. Shaposhnikov, N. Sobolev, V.E. Borisenko, F.A. D’Avitaya, S. Ossicini, *Physical Review B* 70 (2004) 035317.
- [15] A.G. Marinopoulos, L. Reining, A. Rubio, N. Vast, *Physical Review Letters* 91 (2003) 046402.
- [16] E. Chang, G. Bussi, A. Ruini, E. Molinari, *Physical Review Letters* 92 (2004) 196401.

- [17] M. Bruno, M. Palumbo, A. Marini, R.D. Sole, V. Olevano, A.N. Kholod, S. Ossicini, *Physical Review B* 72 (2005) 153310.
- [18] F. Bruneval, S. Botti, L. Reining, *Physical Review Letters* 94 (2005) 219701.
- [19] N. Wang et al., *Nature* 408 (2000) 50.
- [20] D. Kovalev, *Physical Review Letters* 77 (1996) 2089.
- [21] M. Cazzanelli, D. Kovalev, L.D. Negro, Z. Gaburro, L. Pavesi, *Physical Review Letters* 93 (2004) 207402.
- [22] T. Ogawa, T. Takagahara, *Physical Review B* 43 (1991) 14325.
- [23] T. Ogawa, T. Takagahara, *Physical Review B* 44 (1991) 8138.
- [24] S. Ossicini, L. Pavesi, F. Priolo, *Light Emitting Silicon for Micro-photonics*, Springer Tracts in Modern Physics, No. 194, Berlin, 2003.
- [25] Z. Ma, X. Liao, G. Kong, J. Chu, *Applied Physics Letters* 75 (1999) 1857.
- [26] A. Marini, The self software project. Available from: <http://www.fisica.uniroma2.it/~self/>.